Observational Study

Medicine®

OPEN

Effect of HSP27 and Cofilin in the injury of hypoxia/reoxygenation on hepatocyte membrane F-actin microfilaments

Yafei Zhang, MD, Jiazhong Wang, MD, Hong Ji, MD, Hongwei Lu, MD, Le Lu, MD, Jinlong Wang, MD, Yiming Li, MD*

Abstract

Hypoxia–reoxygenation (H/R) injury hepatocyte models were established to simulate the ischemia/reperfusion injury of transplanted organ. Through the study of the molecular mechanism of H/R on the F-actin damage of the liver cytomembrane, the mechanism of F-actin damage induced by ischemia and reperfusion was studied from the level of cell and molecule.

The hypoxic environment of cells in vitro was simulated by chemical hypoxia agent $CoCl_2$. Liver cells were detected by MTT, H/R group was subdivided into 3 subgroups: H/R 2, 4, and 6 h. Changes of cell shape and the growth state, apoptosis, ultrastructural changes, and the changes in F-actin microfilament content were observed. Heat shock protein 27 (HSP27), Cofilin, and F-actin gene and protein levels were determined by real-time polymerase chain reaction and western blot assay, respectively.

Cells showed circular adherence growth under normal circumstances, while the spindle cells and shedding cells were significantly increased in H/R groups. Apoptosis cells in H/R group were increased significantly with the extension of hypoxia time. The number of endoplasmic reticulum was decreased significantly in the H/R group, the mitochondrion hydropic was degenerated and the glycogen was disappeared. The F-actin fibers in the H/R group were disordered, the morphology of the fibers was obviously decreased, and the fluorescence staining decreased obviously ($P < .05$). The transcription and expression levels of HSP27, Cofilin, and F-actin were significantly lower than those in the control group ($P < .05$).

These results demonstrate that H/R can affect the correct assembly of F-actin microfilaments and weakens the normal cycle of F-actin microfilaments through inhibiting the protein expression and gene transcription of HSP27 and Cofilin in hepatocytes, thereby changing the skeleton of F-actin microfilaments.

Abbreviations: H/R = hypoxia–reoxygenation, HSP = heat shock protein, ITBL = ischemic type biliary lesion, PBS = phosphate buffer solution.

Keywords: F-actin, hepatocyte, hypoxia/reoxygenation

1. Introduction

The structure and function of liver is very complex, which has not yet been fully understood. Facing liver disease, a lot of therapeutic methods are helpless, especially the final stage liver disease. Liver disease is the main cause of morbidity and mortality worldwide, constituting a great threat to human health.[1,2]

Previous studies have shown that[3–6] F-actin microfilaments were destructed and the microvilli were loss in the early stage of hepatic artery ischemia reperfusion. However, the morphology and molecular mechanisms of the change in F-actin, microvilli, and hepatocyte have not been reported. Therefore, from the clinical point of view, it is of great significance to understand the molecular mechanism of the abnormal changes of F-actin filaments.

As a small heat shock protein, heat shock protein 27 (HSP27) can mediate the correct assembly of F-actin filament.[7,8] Cofilin can change the structure of F-actin filaments and promote the circulation of F-actin filaments.[9,10] This experiment simulates ischemia reperfusion injury of transplanted organ by establishing hepatocytes in vitro hypoxia/reoxygenation (H/R) injury model. Detecting the gene transcription and protein expression of HSP27 and Cofilin, observing the ultrastructure changes by electron microscope, and observing the content change of F-actin through confocal laser microscope, we are to investigate the mechanism of the injury of F-actin induced by ischemia reperfusion from the cellular and molecular levels.

2. Materials and methods

2.1. Materials

Rat liver cells (BRL-3A) were purchased from the Life Science Institute of Shanghai, Chinese Academy of Sciences, and the treatment of cells was in accordance with ethical standards. Main reagents and instruments used in the experiment as follows: basal medium (Corning, Herndon, Virginia), SYBR Green RT-PCR kit and reverse transcription Kit (Toyobo, Osaka, Japan), Western and IP cell lysis, BCA protein concentration determination kit (Beyotime Biotechnology Research Institute, Shanghai, China),

Editor: Wenyu Lin.

This study was supported by the National Natural Science Foundation of China (NSFC No. 81170454).

The authors have no conflicts of interest to disclose.

Department of General Surgery, The Second Affiliated Hospital of Xi'an Jiaotong University, Xi'an, Shaanxi, China.

* Correspondence: Yiming Li, Department of General Surgery, The Second Affiliated Hospital of Xi'an Jiaotong University, No. 157, Xiwu Road, Xi'an, Shaanxi 710004, China (e-mail: liyimingdoc@163.com).

Medicine (2017) 96:16(e6658)

Received: 27 December 2016 / Received in final form: 28 March 2017 / Accepted: 29 March 2017

http://dx.doi.org/10.1097/MD.0000000000006658

Cofilin, HSP27 monoclonal antibodies (BD, Lake Franklin, New Jersey), GAPDH and TBP polyclonal antibody (Santa Cruz Biotechnology, Inc. Santa Cruz, California), $CoCl_2$ (Sigma, Santa clara, California), FITC-Phalloidin and Anti decay sealing agents (Alexis, New York, NY), and Transmission electron microscope (H-600, HITACHI Company, Tokyo, Japan). Ordinary inverted microscope (TS100, Nikon, Tokyo, Japan) and Laser scanning confocal microscopy (TCS Sp8, Leica, Solms, Germany), real-time quantitative PCR instrument (Stepone, ABI, Carlsbad, California) chemiluminescence gel imaging system (GboxChemi hr16, Syngene, Cambridge, UK) were provided by the Central Laboratory of the Second Affiliated Hospital of Xi'an Jiaotong University. This study had been approved by the Ethics Committee of Xi'an Jiaotong University School of Medicine and was performed in accordance with the Guide for the Care and Use of Laboratory Animals of the Chinese National Institutes of Health. All procedures involving animals were reviewed and approved by the Institutional Animal Care and Use Committee of the Xi'an Jiaotong University (IACUC protocol number: XJTULAC20120026). Patient consent was not applicable in this study for no patient was involved.

2.2. H/R model building

Cells were cultured in 5% CO_2 and 95% O_2 environment routinely. The hypoxic environment in vitro was simulated by chemical hypoxia agent $CoCl_2$ (100 μmol/L). Cell growth inhibition rate was determined using the MTT (Sigma) assay according to the manufacturer's instructions. We found that when the hypoxia time was 3 h, the inhibition rate reached 50%, while the morphological changes of hypoxia in the liver cells occurred under the inverted microscope, such as cell morphology changes gradually from multiangle to circular and elliptical shape, and the gap becomes larger, electron microscopy found mitochondrial swell, more vacuoles occur in the cells, suggesting that the hypoxia model was built successfully. Then the completely DMEM high glucose medium was placed in the incubator (95% air, 5% CO_2) to the corresponding time points.

2.3. Groups

Cells were divided randomly into normal control group and H/R group. H/R group was further divided into H/R 2, 4, and 6 h groups (reoxygenation 2, 4, and 6 h, respectively, after hypoxia 3 h; Fig. 1).

2.4. Growth state of the cells was observed by inverted microscopy

The change of cell shape and the growth state of the cells were observed by inverted microscope.

2.5. Ultrastructural changes of cells were observed by transmission electron microscopy

Reoxygenated BRL-3A cells at different time points were digested by Trypsin and collected, centrifugal to mass, and then produced

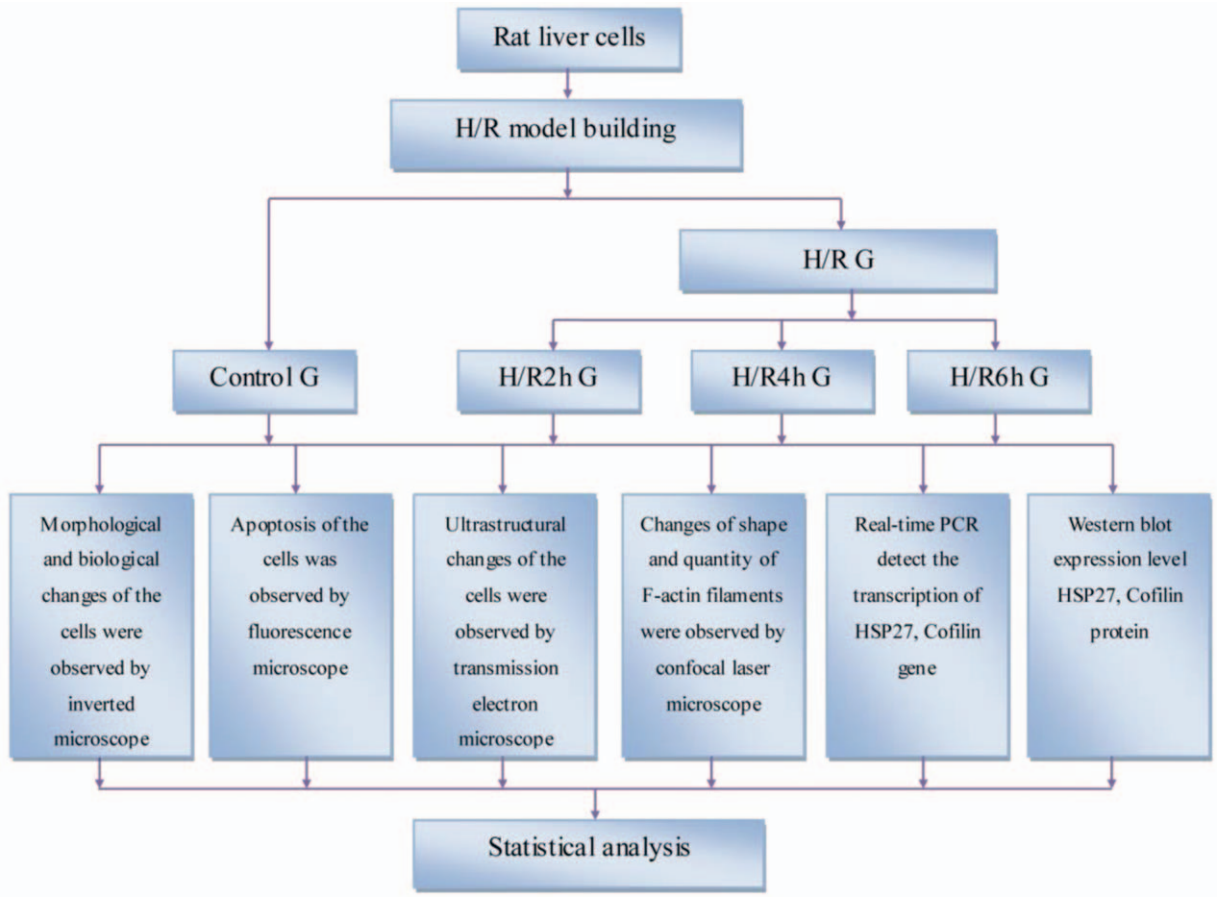

Figure 1. Flow chart of our study.

ultrathin sections of electron microscope and observed ultrastructural changes of cells by transmission electron microscope.

2.6. Apoptotic cells were observed by fluorescence microscope

Prepared cell samples and washed the residual trypsin, disposed upper liquid, gently resuspension cells with the phosphate buffer solution (PBS) 1 mL buffer and count, making the number of cells is >105, then 500g centrifuged 5 min. Add 400 μL 1× binding buffer to gently resuspension cells. Add 10 μL Propidium Iodide (PI), gently mixed evenly, avoid light ice bath 5 min; 1000g centrifuged 5 min, collecting cells, gently resuspension cells with 50 to 100 μL 1× binding buffer, observed and taken pictures with fluorescence microscope after smear. Count the number of apoptotic cells using Image Proplus software.

2.7. F-actin filaments were observed by laser confocal microscopy

Cells were planted on the sterile tablets, rinsed carefully with PBS after 18 h, given corresponding treatment for different groups, then fixed 10 min with 37 g/L polyoxymethylene at room temperature, washed 3 times with PBS; FITC-Phalloidin staining solution (dissolved in methanol, PBS diluted to 10 mg/L) was added avoiding light, incubated 1 h at room temperature, washed 3 times by PBS (15 min every time), mounted by antifluorescent attenuation mounting medium. Finally, observed and acquisited image by laser confocal microscopy, determined the mean-specific fluorescence intensity of liver cytomembrane.

2.8. Real-time quantitative PCR

Total RNA was extracted using Trizol reagent. RNA was reverse-transcribed to cDNA using a reverse transcriptase kit. The relative abundance of each mRNA sample was quantitated by qPCR with specific primers and SYBR Premix Ex Taq. Primers for GAPDH, Cofilin, HSP27, and F-actin were designed and synthesized by Shanghai bio engineering technology services Co., Ltd (Table 1). Real-time polymerase chain reactions (PCRs) were conducted using an iQ Multicolor Real-Time PCR Detection System. Cycle threshold values were obtained from the Bio-Rad iQ5 2.0 Standard Edition optical System software. Data were analyzed using the ΔΔCt method and GAPDH served as an internal control.

2.9. Western blot analysis

Membrane proteins were extracted using the membrane protein extraction kit. Equal amounts of sample were separated using SDS—PAGE. Gels were electroblotted with Sartoblot onto polyvinylidene difluoride membranes. The membranes were blocked in Carnation nonfat milk and probed with a 1:200 dilution of the HSP27, Cofilin, and GAPDH antibodies and a 1:1000 dilution of the second antibody. Antigen/antibody complexes were visualized with a chemiluminescence system and scanned into images. The relative densities of the bands were analyzed using NIH Image. The ratio of target protein to GAPDH served as an index for statistical analysis.

Table 1

Primer sequences of Cofilin, HSP27, F-actin, and β-actin.

Gene	Forward (5′–3′)	Reverse (5′–3′)
GAPDH	AGAAGGCTGGGGCTCATTTG	AGGGGCCATCCACAGTCTTC
Cofilin	CAAGAAGGACCTGGTGTTC	TTGGAGCTGGCGTAGATCATT
HSP27	CGTTGCCAATAACACAAACG	GGCTTCTACTTGGCTCCAGA
F-actin	GCTAAGAAGGCGATACAA	AGAATGAGGACTGGGTGA

2.10. Statistical analysis

All experiments were repeated at least 3 times. Data are expressed as mean ± standard deviation and processed with SPSS 13.0 statistics software (SPSS Inc., Chicago, IL). Differences between 2 groups were assessed by Student *t* test, and 1- or 2-way analysis of variance (ANOVA) with Turkey post hoc test was used for multiple comparisons. Differences were analyzed using ANOVA. A value of $P < .05$ was considered statistically significant.

3. Results

3.1. $CoCl_2$ inhibits the proliferation of liver cells

Cells were treated by $CoCl_2$ with a concentration 100 μmol/L, and the hypoxia time was about 1, 2, 3, 4, 5, and 6 h, respectively. MTT assay found that the inhibition rate was increased in a time-dependent pattern (Fig. 2).

3.2. Cellular morphology changed

Inverted microscope found that cells showed normal circular adherence growth in control group, grew well, showed irregular polygon, and arranged more closely. Liver cells showed different degrees of morphological changes in H/R groups, such as cell shrinkage, cell arranged loosely and the intercellular space widened, fusiform cells increased significantly. With the extension of hypoxia time, exfoliated cells increased significantly and then breaking, disappear (Fig. 3).

3.3. Ultrastructural changed

The cytoplasm of normal liver cells was filled with mitochondria and endoplasmic reticulum. While the number of endoplasmic reticulum was decreased significantly in the H/R group compared with the control group, the mitochondrion hydropic was degenerated and the glycogen was disappeared (Fig. 3).

3.4. Increase of apoptosis

Fluorescence microscope found that only a few cells showed red staining in control group. More cells in H/R were stain red, there

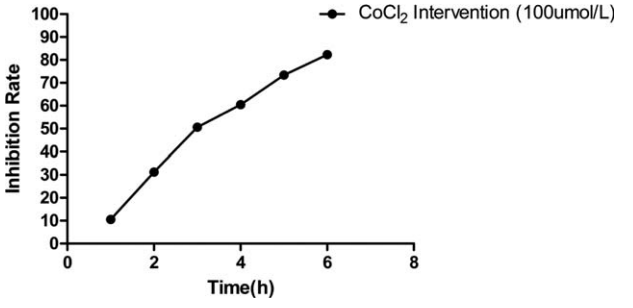

Figure 2. Inhibitory effect of $CoCl_2$ on the proliferation of hepatic cells was detected by MTT. MTT assay found that the inhibition rate was increased in a time-dependent pattern.

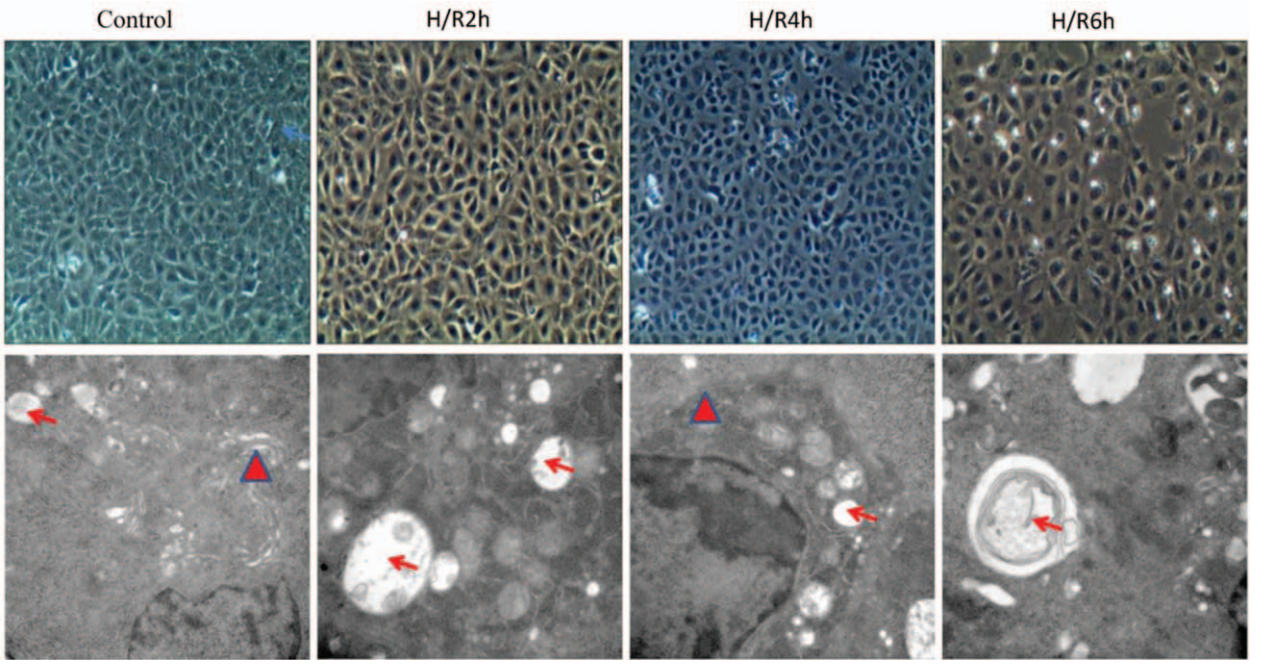

Figure 3. Morphology and ultrastructure changes in each group. Inverted microscope (×100) showed that liver cells grew well in normal circumstances, appeared irregular polygon and the cells arranged closely. While, H/R groups showed cell shrinkage, arranged loosely, intercellular space widened, and fusiform cells increased. With the extension of hypoxia time, exfoliated cells increased significantly and then breaking, disappear. Electron microscopy (×30,000) showed that the cytoplasm of normal liver cells was filled with mitochondria ((➘)) and endoplasmic reticulum ((▲)). While, the number of endoplasmic reticulum was decreased significantly in H/R group and the mitochondrion hydropic was degenerated.

was no obvious background staining. Meanwhile, the negative controls also had no background staining, so the false positive can be excluded. In H/R groups, red nuclei increased significantly ($P < .05$) with the time of reoxygenation, that is, the number of apoptosis cells increased (Fig. 4A and B). By western blot, the expression of cleaved Caspase 3 protein was increased with the extension of hypoxia time, in line with the results of PI staining (Fig. 4D and E).

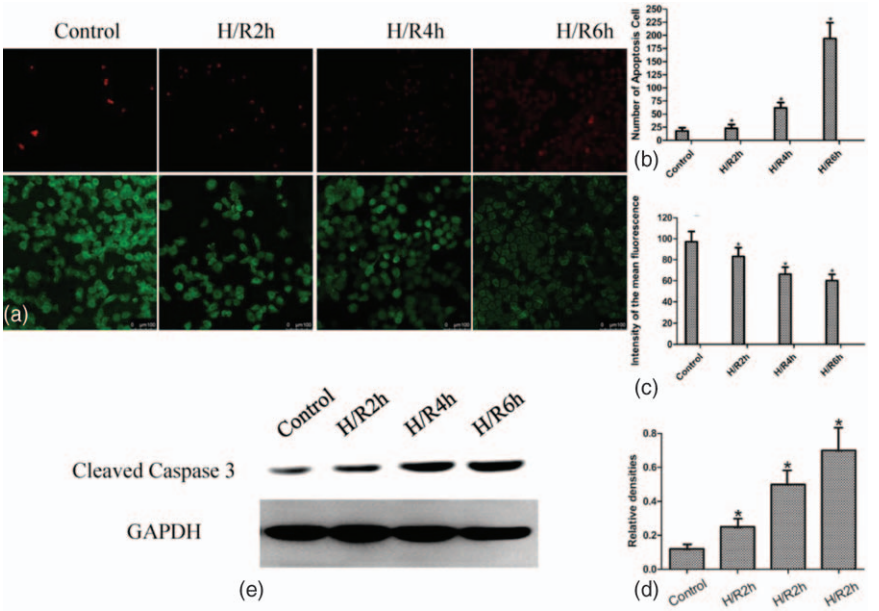

Figure 4. Apoptosis of hepatocytes and the distribution of F-actin. PI staining was used to observe the apoptosis of hepatocytes. Fluorescence microscope (×20) found that only a few cells showed red staining among normal controls. While, most cells in H/R were stained red in H/R groups, which was increased significantly with the time of reoxygenation, that is, the number of apoptosis cells increased significantly ($P < .05$, A, B). By western blot, the expression of cleaved Caspase 3 protein was increased with the extension of hypoxia time, in line with the results of PI staining (D, E). Confocal laser scanning microscopy (×400) showed that the F-actin was densely distributed in cells periphery in control group, with bright fluorescent staining. While, the fluorescence of F-actin fibers in the H/R group was disordered, the morphology of the fibers was obviously changed, and the fluorescence staining decreased obviously. The average fluorescence intensity had significant differences in H/R group and control group ($P < .05$, A, C). *$P < .05$ vs control group. PI = Propidium Iodide.

3.5. Distribution of F-actin filaments decreased

The control group showed that the F-actin was densely distributed in the periphery of the cells, and the fluorescent staining was bright. While the fluorescence of F-actin fibers in the H/R group was disordered, the morphology of the fibers was obviously changed, and the fluorescence staining decreased obviously. The average fluorescence intensity had significant differences in H/R group and control group ($P < .05$, Fig. 4A and C).

3.6. Transcription of HSP27, Cofilin, and F-actin was inhibited

By RT-PCR, the mRNA levels of HSP27, Cofilin, and F-actin in H/R 2, 4, and 6 h group were significantly lower than those of the control group ($P < .05$, Fig. 5A).

3.7. Expression of HSP27, Cofilin, and F-actin was inhibited

By western blot, the expression of HSP27, Cofilin, and F-actin in H/R group was significantly lower than those in control group ($P < .05$, Fig. 5B and C).

4. Discussion

With the successful implementation of the world's first human orthotopic liver transplantation in 1963,[11] the upsurge of liver transplantation was lifted in the world. Presently, liver transplantation has become an important treatment for end-stage liver disease. In recent years, with the improvement of liver transplantation technology and the improvement of the awareness of biliary complications, the biliary anastomotic stenosis due to surgical resection was decreased. However, the high incidence of biliary complications after liver transplantation is still a worldwide problem for liver transplantation.[12,13] Among them, the ischemic type biliary lesion (ITBL) is the major type of biliary complications after liver transplantation, which has greatly affected the long-term survival of recipients. ITBL refers to nonanastomotic stenosis in the biliary tree of the graft liver and appears ischemia imaging change without arterial thrombosis. It may lead to intra- and extra-hepatic biliary stricture, bile duct injury and late graft loss, and is one of the reasons for retransplantation.[14,15] Several risk factors are discussed to be major parameters for the development of ITBL. Among them, prolonged ischemic times, reperfusion injury, disturbance in blood flow through the peribiliary vascular plexus, immunologically induced injury, cytotoxic injury, and ischemia reperfusion injury appear to have the most important influence.[13,16]

There are many canaliculi formed by liver cytomembrane microvilli. Tsukada et al[17] found that bile canaliculi microvilli contains a lot of microfilaments bundles of actin (F-actin), these filaments extending from the plasma membrane to the lumen constitute the inner core of canalicular microvilli. The actin filaments have important role in the bile secretion of bile duct contraction and in maintaining the normal morphology and structure of hepatocytes and bile duct.[18,19] Continuous actin polymerization and depolymerization of F-actin achieve the contraction of bile duct, and then promote the excretion of bile. Loss of the integrity of the actin will result in bile secretion disorders.[3,20,21] Therefore, when various reasons damage the cytoskeleton and lead to the dysfunction of actin filaments, the bile duct contraction is blocked, and then bile duct expansion, resulting in cholestasis.

The establishment of H/R model in our study simulated ischemia reperfusion injury, excluding the effects of hemodynamics, hormone and nerve reflex, can accurately reflect the role of HSP27 and Cofilin in the injury of F-actin. MTT assay found

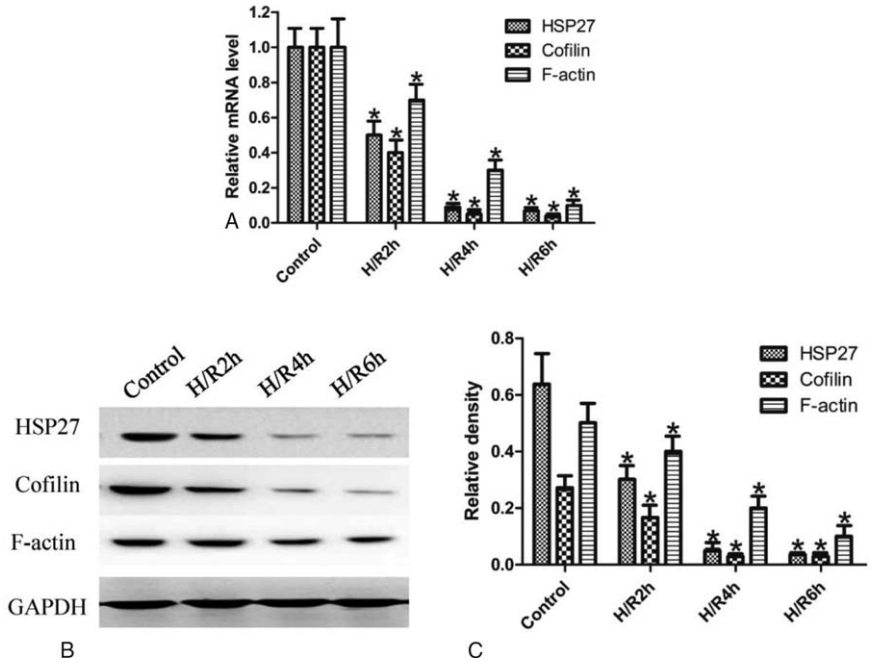

Figure 5. H/R can significantly inhibit the gene transcription and protein expression of HSP27, Cofilin, and F-actin. By RT-PCR, the mRNA levels of HSP27, Cofilin, and F-actin in H/R 2, 4, and 6 h group were significantly lower than those of the control group ($P < .05$, A). By western blot, the expression of HSP27, Cofilin, and F-actin in H/R group was significantly lower than those in control group ($P < .05$, B, C). *$P < .05$ vs control group.

that the inhibition rate increased with the time of hypoxia, having time-dependent pattern, indicating that $CoCl_2$ can well simulate the hypoxia environment of cells in vitro, which were consistent with many research reports.[22–24] Inverted microscope found that cells showed circular adherence growth under normal circumstances, grew well, showed irregular polygon and the cells arranged more closely. While cells showed different degrees of morphological changes in H/R groups, such as cell shrinkage, cell arranged loosely, and intercellular space widened, fusiform cells increased significantly. With the extension of hypoxia time, exfoliated cells increased significantly and then breaking, disappear.

The cytomembrane was intact under normal condition. PI staining found that only a few cells showed red staining in control group, which may result from the normal apoptosis of cells. In H/R groups, red nuclei increased significantly with the time of reoxygenation, that is, the number of apoptosis cells increased. By western blot, the expression of cleaved Caspase 3 protein was increased with the extension of hypoxia time, in line with the results of PI staining. H/R could make ATP enzyme inactivation, energy production, and release barriers, ion pump function is inhibited, intracellular and extracellular ion balance disorder, which leads to the morphological changes and apoptosis of cells. The electron microscopic results showed that the cytoplasm of normal liver cells was full of mitochondria and endoplasmic reticulum, while the number of endoplasmic reticulum decreased significantly in the H/R group compared with the control group, the mitochondrion hydropic degenerated and the glycogen disappeared. The control group showed that the F-actin was densely distributed in the periphery of the cells, and the fluorescent staining was bright. While the fluorescence of F-actin fibers in H/R group was disordered, the morphology of the fibers was obviously changed, and the fluorescence staining decreased obviously. There were significant differences of the average fluorescence intensity in H/R group compared with control group. It was showed that cell activity and the distribution of F-actin were obviously inhibited by H/R, this change is consistent with previous in vivo studies.[25,26]

This experiment used real-time PCR and western blot detect the transcription level and protein expression of HSP27, Cofilin, and F-actin. The current results indicate that the transcription and expression levels of HSP27, Cofilin, and F-actin in H/R 2, 4, and 6 h group were significantly lower than those in control group, and with the prolongation of reperfusion time, the transcription and expression levels of the trend were decreased, indicating that the transcription and expression of HSP27, Cofilin, and F-actin were obviously inhibited by H/R, which were consistent with changes of fluorescence and ultrastructural of electron microscope in this experiment. It is suggested that the alterations of HSP27 and Cofilin activity may be an effective mechanism for the damage of F-actin filaments in the membrane of the H/R cells.

The process of actin polymerization can be divided into 4 steps: actin monomer activation; actin monomer polymerization nucleation; actin filament growth; and polymerization achieves dynamic equilibrium.[5,6] HSP27 is a kind of small heat shock protein, whose expression can be induced by cellular stress stimulation and can mediate the correct assembly of actin as molecular chaperone. The regulatory mechanism HSP27 is dependent on the expression of its proteins and phosphorylated proteins. Phosphorylated HSP27 is an active form of cellular protection function. However, the phosphorylation of HSP27 will destroy its structure and make it lose the function of molecular chaperone.[7,27] Physiological levels of oxygen free radicals are necessary for life, but large amounts of oxygen free radicals may lead to irreversible cell damage and cell death.[28] Experiments have proved that in the animal nonskeletal muscle cells, oxygen free radicals can make actin polymerization regulator (HSP27) phosphorylated through activating the mitogen-activated protein kinase (especially protein kinase 2/P38). As a result, the structure of actin cytoskeleton was changed obviously.[29] As we all know, H/R can produce more oxygen free radicals.[30] In this experiment, we hypothesized that liver cells produced a large amount of oxygen free radicals after H/R, lead to the phosphorylation of HSP27, causes it lose the function of molecular chaperones, thereby causing the changes of the F-actin cytoskeleton structure (Fig. 6).

In addition, Cofilin is also important factor to regulate cytoskeletal remodeling. Cofilin can bind to actin filaments or actin monomers, its main function is to decompose the actin filaments and increase the dissociation speed of the actin monomer from end of the actin filaments, so as to promote the cycle of actin microfilaments.[31] The activity of Cofilin depends on the phosphorylation and dephosphorylation of N terminal Ser-3 sites.[32] Previous research has shown that oxidative stress can promote the phosphorylation of Cofilin in endothelial cells and inhibit the activity of Cofilin, thus it can affect the polymerization of actin.[33] We speculate that oxidative stress can promote the phosphorylation of Cofilin in hepatocytes after H/R, thereby weaken the function of decomposing actin filaments, decreased the dissociation speed of the actin monomer from end of the actin filaments, affect the normal cycle of the actin filament, so as to cause the changes in the F-actin cytoskeleton structure (Fig. 6).

In conclusion, H/R can enhance the phosphorylation of HSP27 and Cofilin in liver cells, affect the biological activity of Cofilin and HSP27, thus affect the correct assembly of F-actin and weaken the normal circulation of F-actin, and then change the normal cytoskeleton of F-actin microfilaments. Cell experiments excluded hemodynamics, hormone, and nerve reflex can accurately reflect the role of HSP27 and Cofilin in the injury of F-actin and the effective mechanism of F-actin injury, which can better explain the ischemia reperfusion injury of F-actin in vivo, thus further guide clinical work.

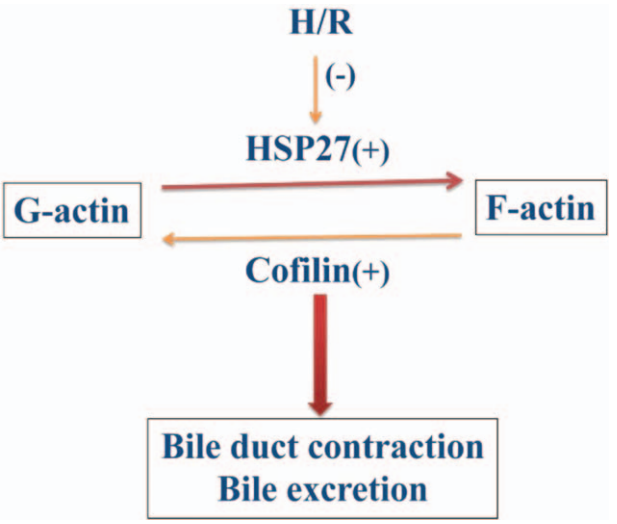

Figure 6. Schematic diagram. H/R = hypoxia–reoxygenation.

References

[1] Greco E, Nanji S, Bromberg IL, et al. Predictors of peri-opertative morbidity and liver dysfunction after hepatic resection in patients with chronic liver disease. HPB 2011;13:559–65.

[2] El-Karaksy HM, El-Shabrawi MM, Mohsen NA, et al. Study of predictive value of pediatric risk of mortality (PRISM) score in children with end stage liver disease and fulminant hepatic failure. Indian J Pediatr 2011;78:301–6.

[3] Nieuwenhuijs VB, De Bruijn MT, Padbury RT, et al. Hepatic ischemia-reperfusion injury: roles of Ca^{2+} and other intracellular mediators of impaired bile flow and hepatocyte damage. Dig Dis Sci 2006;51: 1087–102.

[4] van der Heijden M, Versteilen AMG, Sipkema P, et al. Rho-kinase-dependent F-actin rearrangement is involved in the inhibition of PI3-kinase/Akt during ischemia-reperfusion-induced endothelial cell apoptosis. Apoptosis 2008;13:404–12.

[5] Hutchins BI, Klenke U, Wray S. Calcium release-dependent actin flow in the leading process mediates axophilic migration. J Neurosci 2013;33: 11361–71.

[6] Ritchey L, Chakrabarti R. Aurora A kinase modulates actin cytoskeleton through phosphorylation of Cofilin: implication in the mitotic process. BBA Mol Cell Res 2014;1843:2719–29.

[7] Huang J, Xie LD, Luo L, et al. Silencing heat shock protein 27 (HSP27) inhibits the proliferation and migration of vascular smooth muscle cells in vitro. Mol Cell Biochem 2014;390:115–21.

[8] Kostenko S, Johannessen M, Moens U. PKA-induced F-actin rearrangement requires phosphorylation of HSP27 by the MAPKAP kinase MK5. Cell Signal 2009;21:712–8.

[9] Anne OS, Bernheim-Groswasser A. Reconstitution of actin-based motility by vasodilator-stimulated phosphoprotein (VASP) depends on the recruitment of F-actin seeds from the solution produced by Cofilin. J Biol Chem 2014;289:31274–86.

[10] Chen CK, Benchaar SA, Phan M, et al. Cofilin-induced changes in F-actin detected via cross-linking with benzophenone-4-maleimide. Biochemistry 2013;52:5503–9.

[11] Starzl TE, Marchioro TL, Vonkaulla KN, et al. Homotransplantation of the liver in humans. Surg Gynecol Obstet 1963;117:659–76.

[12] Hansen T, Hollemann D, Pitton MB, et al. Histological examination and evaluation of donor bile ducts received during orthotopic liver transplantation—a morphological clue to ischemic-type biliary lesion? Virchows Arch 2012;461:41–8.

[13] Jin X, Shi XJ, Wang MQ, et al. Causes and management of ischemic-type biliary lesion after orthotopic liver transplantation. Zhonghua Yi Xue Za Zhi 2011;91:251–5.

[14] Bang JB, Kim BW, Kim YB, et al. Risk factor for ischemic-type biliary lesion after ABO-incompatible living donor liver transplantation. World J Gastroenterol 2016;22:6925–35.

[15] Scanga AE, Kowdley KV. Management of biliary complications following orthotopic liver transplantation. Curr Gastroenterol Rep 2007;9:31–8.

[16] Farid WRR, de Jonge J, Zondervan PE, et al. Relationship between the histological appearance of the portal vein and development of ischemic-type biliary lesions after liver transplantation. Liver Transplant 2013; 19:1088–98.

[17] Tsukada N, Ackerley CA, Phillips MJ. The structure and organization of the bile canalicular cytoskeleton with special reference to actin and actin-binding proteins. Hepatology 1995;21:1106–13.

[18] Yi-ming LI, Ji-dong LIU, Hong JI, et al. Effect of ischemia-reperfusion on bile canalicular F-actin microfilaments in rat liver. J Xi'an Jiaotong Univ Med Sci 2009;30:210–3.

[19] Benkoel L, Dodero F, Hardwigsen J, et al. Effect of ischemia-reperfusion on bile canalicular F-actin microfilaments in hepatocytes of human liver allograft: image analysis by confocal laser scanning microscopy. Dig Dis Sci 2001;46:1663–7.

[20] Nagai H, Kato A, Kimura F, et al. Endothelin-1 aggravates hepatic ischemia/reperfusion injury during obstructive cholestasis in bile duct ligated mice. J Surg Res 2010;162:46–53.

[21] Sudo R, Kohara H, Mitaka T, et al. Coordinated movement of bile canalicular networks reconstructed by rat small hepatocytes. Ann Biomed Eng 2005;33:696–708.

[22] Dai ZJ, Gao J, Ma XB, et al. Up-regulation of hypoxia inducible factor-1alpha by cobalt chloride correlates with proliferation and apoptosis in PC-2 cells. J Exp Clin Cancer Res 2012;31:28.

[23] Torii S, Kurihara A, Li XY, et al. Inhibitory effect of extracellular histidine on cobalt-induced HIF-1alpha expression. J Biochem 2011; 149:171–6.

[24] Zhong X, Lin R, Li Z, et al. Effects of Salidroside on cobalt chloride-induced hypoxia damage and mTOR signaling repression in PC12 cells. Biol Pharm Bull 2014;37:1199–206.

[25] Wang JZ, Liu Y, Wang JL, et al. Hepatic artery bridging lessens temporary ischemic injury to bile canaliculi. World J Gastroenterol 2015;21:10113–25.

[26] Liu Y, Wang J, Yang P, et al. Delayed rearterialization unlikely leads to nonanastomotic stricture but causes temporary injury on bile duct after liver transplantation. Transplant Int 2015;28:341–51.

[27] Sun Y, Meng GM, Guo ZL, et al. Regulation of heat shock protein 27 phosphorylation during microcystin-LR-induced cytoskeletal reorganization in a human liver cell line. Toxicol Lett 2011;207:270–7.

[28] Hambarde S, Singh V, Chandna S. Evidence for involvement of cytosolic thioredoxin peroxidase in the excessive resistance of Sf9 Lepidopteran insect cells against radiation-induced apoptosis. PLoS ONE 2013;8: e58261.

[29] Evertsson K, Fjallstrom AK, Norrby M, et al. p38 mitogen-activated protein kinase and mitogen-activated protein kinase-activated protein kinase 2 (MK2) signaling in atrophic and hypertrophic denervated mouse skeletal muscle. J Mol Signal 2014;9:2.

[30] Collins P, Jones C, Choudhury S, et al. Increased expression of uncoupling protein 2 in HepG2 cells attenuates oxidative damage and apoptosis. Liver Int 2005;25:880–7.

[31] Huh YH, Kim SH, Chung KH, et al. Swiprosin-1 modulates actin dynamics by regulating the F-actin accessibility to Cofilin. Cell Mol Life Sci 2013;70:4841–54.

[32] Lian JP, Marks PG, Wang JY, et al. A protein kinase from neutrophils that specifically recognizes Ser-3 in Cofilin. J Biol Chem 2000;275: 2869–76.

[33] Hsieh YC, Rao YK, Wu CC, et al. Methyl anteinate A from antrodia camphorata induces apoptosis in human liver cancer cells through oxidant-mediated Cofillin- and Bax-triggered mitochondrial pathway. Chem Res Toxicol 2010;23:1256–67.